

# Strong first order S-ROCK methods for stochastic differential equations

著者	Komori Y., Burrage K.
journal or publication title	Journal of Computational and Applied Mathematics
volume	242
page range	261-274
year	2012-11-01
URL	<a href="http://hdl.handle.net/10228/5878">http://hdl.handle.net/10228/5878</a>

doi: 10.1016/j.cam.2012.10.026

# Strong first order S-ROCK methods for stochastic differential equations

Yoshio Komori<sup>a</sup>, Kevin Burrage<sup>b,c</sup>

<sup>a</sup>*Department of Systems Design and Informatics, Kyushu Institute of Technology, Iizuka 820-8502, Japan*

<sup>b</sup>*Department of Computer Science, University of Oxford, Wolfson Building, Parks Road, Oxford, OX1 3QD, UK*

<sup>c</sup>*Discipline of Mathematics, Queensland University of Technology, Brisbane, QLD 4001, Australia*

---

## Abstract

Explicit stochastic Runge-Kutta (SRK) methods are constructed for non-commutative Itô and Stratonovich stochastic differential equations. Our aim is to derive explicit SRK schemes of strong order one, which are derivative free and which have large stability regions. In the present paper, this will be achieved by embedding Chebyshev methods for ordinary differential equations in SRK methods proposed by Rößler (2010). In order to check their convergence order, stability properties and computational efficiency, some numerical experiments will be performed.

*Keywords:* Explicit method, Mean square stability, Stochastic orthogonal Runge-Kutta Chebyshev method

*2008 MSC:* 60H10, 65L05, 65L06

---

## 1. Introduction

While it has been customary to treat the numerical solution of stiff ordinary differential equations (ODEs) by implicit methods, there is a class of explicit methods with extended stability regions that are well suited to solving stiff problems whose eigenvalues lie near the negative real axis. An original contribution is by van der Houwen and Sommeijer [1] who have constructed

---

*Email addresses:* `komori@ces.kyutech.ac.jp` (Yoshio Komori),  
`kevin.burrage@cs.ox.ac.uk`, `kevin.burrage@gmail.com` (Kevin Burrage)

explicit  $s$ -stage Runge-Kutta (RK) methods whose stability functions are shifted Chebyshev polynomials  $T_s(1 + z/s^2)$ . These have stability regions along the negative real axis of  $[-2s^2, 0]$ . The corresponding RK methods satisfy a three term recurrence relation that make them efficient to implement. Such ideas have been developed by Abdulle and Medovikov [2] to construct second order Chebyshev methods with a nearly optimal stability region, which also satisfy a three term recurrence relation. At the same time, in order to avoid the fact that the stability region can collapse to  $s - 1$  single points on the negative real axis, they have introduced a damping factor  $\eta < 1$  by which the modulus of the stability polynomial is bounded, and have proposed second order Chebyshev methods with a damping factor  $\eta$ . When  $\eta = 0.95$ , the stability region for a given  $s$  is along the negative real axis  $[-l_s, -\varepsilon]$ , where  $l_s \approx 0.81s^2$  and  $\varepsilon$  is a small positive value.

In the case of stochastic differential equations (SDEs) the issues are much more complicated. Nevertheless, Abdulle and Cirilli [3] have developed a family of explicit stochastic orthogonal Runge-Kutta Chebyshev (SROCK) methods with extended mean square (MS) stability regions. These methods are of strong order a half for non-commutative Stratonovich SDEs. Abdulle and Li [4] have proposed SROCK methods of the same order for non-commutative Itô SDEs. Both of them reduce to the first order Chebyshev methods when they are applied to ODEs. Such approaches are important because implicit or drift-implicit stochastic Runge-Kutta (SRK) methods [5, 6, 7, 8, 9] lead to solving a large nonlinear system of equations when the dimension of SDEs is large. Despite the claimed performance of the SROCK methods, there is still a drawback. It is the low convergence order.

We are concerned with strong first order methods, especially derivative-free ones, for non-commutative SDEs. Burrage and Burrage [10] have given a general framework for deriving order conditions for SRK methods for Stratonovich SDEs. It generalizes the rooted tree theory of Butcher [11] by having  $m + 1$  colored nodes of a tree when the stochastic differential equation (SDE) is driven by an  $m$ -dimensional Wiener process. Rößler [12] has used this rooted tree theory to construct strong first order SRK methods with significantly reduced computational complexity for non-commutative Itô and Stratonovich SDEs. In addition, Wiktorsson [13] has proposed efficient approximations to double stochastic integrals, which are necessary in methods of strong order one for non-commutative SDEs.

In a similar situation the present authors extended these ideas for weak order SRK methods and succeeded in deriving new SROCK methods with high

weak order [14]. In the present paper we shall put all these ideas together. On the basis of Rößler's SRK family, we will derive  $s$ -stage SRK schemes that are of strong order one for non-commutative Itô and Stratonovich SDEs and which have extended MS stability regions. The schemes will reduce to the first or second order Chebyshev methods when they are applied to ODEs. In Section 2 we will introduce Chebyshev methods for ODEs. In Section 3 we will derive our SRK methods, and in Section 4 we will give their stability analysis. Section 5 will present numerical results and Section 6 our concluding remarks.

## 2. Chebyshev methods for ODEs

For the autonomous  $d$ -dimensional ordinary differential equation (ODE)

$$\mathbf{y}'(t) = \mathbf{f}(\mathbf{y}(t)), \quad t > 0, \quad \mathbf{y}(0) = \mathbf{y}_0, \quad (1)$$

explicit RK methods with  $s$  stages are given by

$$\mathbf{H}_i^{(0)} = \mathbf{y}_n + h \sum_{j=1}^{i-1} a_{ij} \mathbf{f}(\mathbf{H}_j^{(0)}) \quad (1 \leq i \leq s), \quad \mathbf{y}_{n+1} = \mathbf{y}_n + h \sum_{j=1}^s b_j \mathbf{f}(\mathbf{H}_j^{(0)}). \quad (2)$$

Here, for an equidistant grid point  $t_n \stackrel{\text{def}}{=} nh$  ( $n = 1, 2, \dots, M$ ) with step size  $h$  ( $M$  is a natural number),  $\mathbf{y}_n$  denotes a discrete approximation to the solution  $\mathbf{y}(t_n)$  of (1).

When we apply (2) to the scalar test equation

$$y'(t) = \lambda y(t), \quad t > 0, \quad y(0) = y_0, \quad (3)$$

where  $\Re(\lambda) \leq 0$  and  $y_0 \neq 0$ , we have  $y_{n+1} = R_s(h\lambda)y_n$ . Here,  $R_s(z)$  is called a stability function and is expressed by

$$R_s(z) = 1 + \sum_{j=1}^s z^j \mathbf{b}^\top A^{j-1} \mathbf{e}, \quad (4)$$

where  $A$  is an  $s \times s$  matrix  $[a_{ij}]$ ,  $\mathbf{b} \stackrel{\text{def}}{=} [b_1 \ b_2 \ \dots \ b_s]^\top$  and  $\mathbf{e} \stackrel{\text{def}}{=} [1 \ 1 \ \dots \ 1]^\top$ . In addition,  $S \stackrel{\text{def}}{=} \{z \mid |R_s(z)| \leq 1\}$  is called the A-stability region of (2).

The Chebyshev methods are categorized into a class of explicit RK methods.



### 2.1. Chebyshev methods of order one (ROCK1 methods)

Van der Houwen and Sommeijer [1] have constructed RK methods of order one which have the maximal stability region along the negative real axis  $[-2s^2, 0]$ . These methods have the maximal stability polynomial given by

$$R_s(z) = T_s\left(1 + \frac{z}{s^2}\right), \quad (5)$$

where  $T_k(x)$  is the Chebyshev polynomial of degree  $k$  defined by  $T_k(\cos \theta) \stackrel{\text{def}}{=} \cos(k\theta)$  or by the three term recurrence relation

$$T_0(x) \stackrel{\text{def}}{=} 1, \quad T_1(x) \stackrel{\text{def}}{=} x, \quad T_k(x) \stackrel{\text{def}}{=} 2xT_{k-1}(x) - T_{k-2}(x), \quad k \geq 2.$$

The corresponding RK method that has the stability function (5) can be written as the following three term recurrence relation:

$$\begin{aligned} K_0 &\stackrel{\text{def}}{=} \mathbf{y}_n, & K_1 &\stackrel{\text{def}}{=} \mathbf{y}_n + \frac{h}{s^2} \mathbf{f}(K_0), \\ K_j &\stackrel{\text{def}}{=} 2\frac{h}{s^2} \mathbf{f}(K_{j-1}) + 2K_{j-1} - K_{j-2} \quad (2 \leq j \leq s), & \mathbf{y}_{n+1} &= K_s. \end{aligned} \quad (6)$$

One of the drawbacks associated with this family of methods is that the stability region reduces to a single point at  $s = 1$  intermediate points in  $[-2s^2, 0]$ . This can be overcome by introducing a damping parameter  $\eta_1$  which allows a strip around the negative real axis to be included in the stability region at a cost of a slightly shortening of the stability interval. This can be achieved by setting

$$R_s(z) = P_s(z) \stackrel{\text{def}}{=} \frac{T_s(\omega_0 + \omega_1 z)}{T_s(\omega_0)}, \quad \omega_0 \stackrel{\text{def}}{=} 1 + \frac{\eta_1}{s^2}, \quad \omega_1 \stackrel{\text{def}}{=} \frac{T_s(\omega_0)}{T'_s(\omega_0)}. \quad (7)$$

See Figure 1. We will refer to  $P_s(z)$  in later sections.

The corresponding RK method can be written as the following three term recurrence relation:

$$\begin{aligned} K_0 &\stackrel{\text{def}}{=} \mathbf{y}_n, & K_1 &\stackrel{\text{def}}{=} \mathbf{y}_n + h \frac{\omega_1}{\omega_0} \mathbf{f}(K_0), \\ K_j &\stackrel{\text{def}}{=} 2 \frac{T_{j-1}(\omega_0)}{T_j(\omega_0)} (h\omega_1 \mathbf{f}(K_{j-1}) + \omega_0 K_{j-1}) - \frac{T_{j-2}(\omega_0)}{T_j(\omega_0)} K_{j-2} \quad (2 \leq j \leq s), & (8) \\ \mathbf{y}_{n+1} &= K_s. \end{aligned}$$

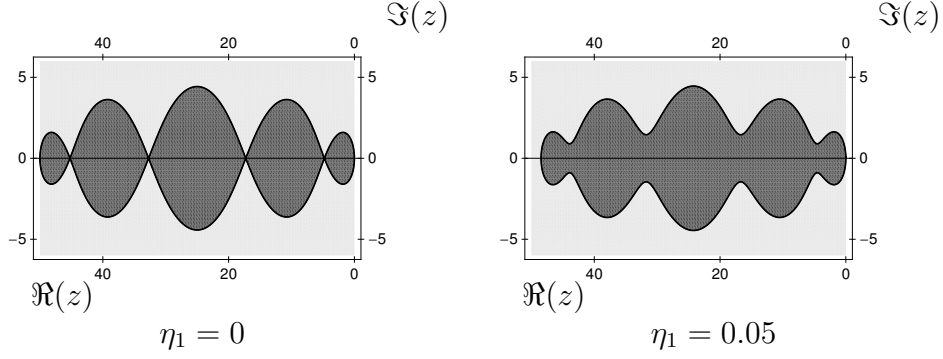


Figure 1: Stability region for  $s = 5$  and  $\eta_1 = 0, 0.05$

## 2.2. Chebyshev methods of order two (ROCK2 methods)

Now, let us require

$$R_s(z) = 1 + z + \frac{1}{2}z^2 + \sum_{j=3}^s c_{s,j}z^j$$

such that  $|R_s(z)| \leq 1$  for  $z \in [-l_s, 0]$  with  $l_s$  as large as possible, where  $c_{s,j} \in \mathbf{R}$ . Riha [15] has shown that such polynomials uniquely exist (for all degrees  $s$ ), satisfy an equal ripple property on  $s - 1$  points and have exactly two complex zeros. Abdulle and Medovikov [2] have constructed the following approximations to these optimal stability polynomials:

$$R_s(x) = w(x)Q_{s-2}(x), \quad w(x) \stackrel{\text{def}}{=} \bar{w}(a_s + x/d_s), \quad Q_j(x) \stackrel{\text{def}}{=} \bar{Q}_j(a_s + x/d_s),$$

where  $a_s, d_s > 0$ ,  $\bar{w}(x)$  is of degree two with complex zeros and satisfies  $\bar{w}(a_s) = 1$ , and where  $\bar{Q}_0(x), \bar{Q}_1(x), \dots, \bar{Q}_{s-2}(x)$  are orthogonal with respect to the weight function  $\bar{w}^2(x)/\sqrt{1-x^2}$  on  $[-1, 1]$ ,  $\bar{Q}_0(a_s) = \bar{Q}_1(a_s) = \dots = \bar{Q}_{s-2}(a_s) = 1$ , and they satisfy a three term recurrence relation. This leads to the method

$$\begin{aligned} K_0 &\stackrel{\text{def}}{=} \mathbf{y}_n, & K_1 &\stackrel{\text{def}}{=} \mathbf{y}_n + h\mu_1 \mathbf{f}(K_0), \\ K_j &\stackrel{\text{def}}{=} h\mu_j \mathbf{f}(K_{j-1}) + (\kappa_j + 1)K_{j-1} - \kappa_j K_{j-2} \quad (2 \leq j \leq s-2), \\ K_{s-1} &\stackrel{\text{def}}{=} K_{s-2} + h\theta_s \mathbf{f}(K_{s-2}), & K_s^* &\stackrel{\text{def}}{=} K_{s-1} + h\theta_s \mathbf{f}(K_{s-1}), \\ K_s &\stackrel{\text{def}}{=} K_s^* - h\theta_s \left(1 - \frac{\tau_s}{\theta_s^2}\right) (\mathbf{f}(K_{s-1}) - \mathbf{f}(K_{s-2})), & \mathbf{y}_{n+1} &= K_s, \end{aligned} \tag{9}$$

where  $\mu_j$ ,  $\kappa_j$ ,  $\theta_s$  and  $\tau_s$  are parameters and they will be defined later.

The computation of  $K_{s-1}$ ,  $K_s^*$  can be viewed as a finishing procedure. If (9) is applied to (3), then

$$K_j = Q_j(z)y_n \quad (0 \leq j \leq s-2), \quad K_s = w(z)K_{s-2}, \quad y_{n+1} = R_s(z)y_n,$$

where

$$w(z) = 1 + 2\theta_s z + \tau_s z^2 \quad (10)$$

and

$$\begin{aligned} Q_0(z) &= 1, & Q_1(z) &= 1 + \mu_1 z, \\ Q_j(z) &= (\mu_j z + \kappa_j + 1)Q_{j-1}(z) - \kappa_j Q_{j-2}(z) \quad (2 \leq j \leq s-2). \end{aligned} \quad (11)$$

If the zeros of  $w$  are  $\alpha_s + i\beta_s$  and  $\alpha_s - i\beta_s$ , then

$$\theta_s = \frac{a_s - \alpha_s}{d_s((a_s - \alpha_s)^2 + \beta_s^2)}, \quad \tau_s = \frac{1}{d_s^2((a_s - \alpha_s)^2 + \beta_s^2)}, \quad d_s = \frac{l_s}{1 + a_s}.$$

The value of  $l_s$  depends on the damping in (9). Away from  $z = 0$  it is appropriate to require  $|R_s(z)| \leq \eta_2 < 1$  for  $z \leq -\varepsilon$  ( $\varepsilon$  : a small positive parameter), whereas we allow  $\eta_2 \leq |R_s(z)| \leq 1$  for  $z \in [-\varepsilon, 0]$ . A number of authors set  $\eta_2 = 0.95$ . In this case the value of  $l_s$  is approximately equal to  $0.81s^2$  (rather than  $0.82s^2$  for  $\eta_2 = 1$ ). Finally, we can determine the values of  $\mu_j$  and  $\kappa_j$  by inserting two different nonzero values, say  $r_1$  and  $r_2$ , into  $z$  in (11) and solving

$$(\mu_j r_i + \kappa_j + 1)Q_{j-1}(r_i) - \kappa_j Q_{j-2}(r_i) = Q_j(r_i), \quad i = 1, 2$$

under the assumption that the system is non-singular [2].

### 3. SRK methods

Consider the autonomous  $d$ -dimensional SDE

$$d\mathbf{y}(t) = \mathbf{f}(\mathbf{y}(t))dt + \sum_{j=1}^m \mathbf{g}_j(\mathbf{y}(t))dW_j(t), \quad t > 0, \quad \mathbf{y}(0) = \mathbf{y}_0, \quad (12)$$

where the  $W_j(t)$ ,  $j = 1, 2, \dots, m$  are independent Wiener processes and  $\mathbf{y}_0$  is independent of  $W_j(t) - W_j(0)$  for  $t > 0$ . If a global Lipschitz condition is

satisfied, the SDE has exactly one continuous global solution on the entire interval  $[0, \infty)$  [16, p. 113].

For (12) we deal with a simpler version of the SRK methods proposed by Rößler [12], that is,

$$\begin{aligned} \mathbf{H}_{i_a}^{(0)} &= \mathbf{y}_n + \sum_{i_b=1}^{i_a-1} A_{i_a i_b}^{(0)} h \mathbf{f} \left( \mathbf{H}_{i_b}^{(0)} \right), \\ \mathbf{H}_{i_a}^{(j)} &= \mathbf{y}_n + \sum_{i_b=1}^s A_{i_a i_b}^{(1)} h \mathbf{f} \left( \mathbf{H}_{i_b}^{(0)} \right) + \sum_{i_b=1}^{i_a-1} \sum_{l=1}^m B_{i_a i_b}^{(1)} \tilde{\zeta}^{(l,j)} \mathbf{g}_l \left( \mathbf{H}_{i_b}^{(l)} \right), \\ \mathbf{y}_{n+1} &= \mathbf{y}_n + \sum_{i=1}^s \alpha_i h \mathbf{f} \left( \mathbf{H}_i^{(0)} \right) + \sum_{i=1}^s \sum_{j=1}^m \left( \beta_i^{(1)} \Delta W_j + \beta_i^{(2)} \sqrt{h} \right) \mathbf{g}_j \left( \mathbf{H}_i^{(j)} \right), \end{aligned} \tag{13}$$

where  $\Delta W_j \stackrel{\text{def}}{=} W_j(t_n + h) - W_j(t_n)$ ,

$$\tilde{\zeta}^{(j,j)} \stackrel{\text{def}}{=} \begin{cases} \frac{1}{2\sqrt{h}} ((\Delta W_j)^2 - h) & \text{(for Itô SDEs),} \\ \frac{1}{2\sqrt{h}} (\Delta W_j)^2 & \text{(for Stratonovich SDEs),} \end{cases} \tag{14}$$

and

$$\tilde{\zeta}^{(l,j)} \stackrel{\text{def}}{=} \frac{1}{\sqrt{h}} \int_{t_n}^{t_{n+1}} (W_l(u) - W_l(t_n)) dW_j(u) \quad (j \neq l).$$

Note that all the parameters  $B_{i_a i_b}^{(0)}$  in [12] are set at zero in the version above. This is due to good stability properties, and also it is remarkable that they do not contribute to any order conditions for strong order one. The definition in (14) decides whether (13) is for Itô or Stratonovich SDEs.

In general, when discrete approximations  $\mathbf{y}_n$  are given by a scheme, we say that the scheme is of strong order  $p$  if there exists a constant  $C$  such that

$$(E[||\mathbf{y}_M - \mathbf{y}(T)||^2])^{1/2} \leq Ch^p$$

with  $T = Mh$  and  $h$  sufficiently small [7, 12].

Let us assume  $\mathbf{f}, \mathbf{g}_j \in \mathbf{C}^3$  for  $j = 1, 2, \dots, m$ . Then, the order conditions

for strong order one are given as follows [12]:

$$\begin{aligned}
1. \quad & \sum_{i=1}^s \alpha_i = 1, & 2. \quad & \sum_{i=1}^s \beta_i^{(1)} = 1, & 3. \quad & \sum_{i=1}^s \beta_i^{(2)} = 0, \\
4. \quad & \sum_{i_a=1}^s \beta_{i_a}^{(1)} \sum_{i_b=1}^{i_a-1} B_{i_a i_b}^{(1)} = 0, & 5. \quad & \sum_{i_a=1}^s \beta_{i_a}^{(2)} \sum_{i_b=1}^{i_a-1} B_{i_a i_b}^{(1)} = 1, & 6. \quad & \sum_{i_a=1}^s \beta_{i_a}^{(2)} \sum_{i_b=1}^s A_{i_a i_b}^{(1)} = 0, \\
7. \quad & \sum_{i_a=1}^s \beta_{i_a}^{(2)} \left( \sum_{i_b=1}^{i_a-1} B_{i_a i_b}^{(1)} \right)^2 = 0, & 8. \quad & \sum_{i_a=1}^s \beta_{i_a}^{(2)} \sum_{i_b=1}^{i_a-1} B_{i_a i_b}^{(1)} \sum_{i_c=1}^{i_b-1} B_{i_b i_c}^{(1)} = 0.
\end{aligned}$$

In the sequel, we will make the number of nonzero roles concerning the stochastic components as small as possible. For this, we suppose

$$B_{i_a i_b}^{(1)} = 0, \quad \beta_{i_b}^{(1)} = \beta_{i_b}^{(2)} = 0 \quad (15)$$

for  $i_a \leq s-2$  or  $i_b \leq s-3$ . Then, since  $\mathbf{H}_1^{(j)}, \mathbf{H}_2^{(j)}, \dots, \mathbf{H}_{s-3}^{(j)}$  are not necessary in (13), we can make  $A_{i_a i_b}^{(1)}$  zero for  $i_a \leq s-3$ . In addition,  $A_{i_a i_b}^{(0)} = B_{i_a i_b}^{(1)} = 0$  ( $i_a \leq i_b$ ) because the methods are explicit. From Conditions 3, 5, 7 and 8 we obtain

$$\begin{aligned}
\beta_{s-2}^{(2)} &= -\frac{B_{s-1, s-2}^{(1)} + B_{s, s-2}^{(1)}}{B_{s-1, s-2}^{(1)} B_{s, s-2}^{(1)}}, & \beta_{s-1}^{(2)} &= -\frac{B_{s, s-2}^{(1)}}{B_{s-1, s-2}^{(1)} (B_{s-1, s-2}^{(1)} - B_{s, s-2}^{(1)})}, \\
\beta_s^{(2)} &= \frac{B_{s-1, s-2}^{(1)}}{B_{s, s-2}^{(1)} (B_{s-1, s-2}^{(1)} - B_{s, s-2}^{(1)})}, & B_{s, s-1}^{(1)} &= 0.
\end{aligned} \quad (16)$$

Substituting the last equation into Condition 4, we have

$$\beta_{s-1}^{(1)} = -\frac{B_{s, s-2}^{(1)} (1 - \beta_{s-2}^{(1)})}{B_{s-1, s-2}^{(1)} - B_{s, s-2}^{(1)}}, \quad \beta_s^{(1)} = \frac{B_{s-1, s-2}^{(1)} (1 - \beta_{s-2}^{(1)})}{B_{s-1, s-2}^{(1)} - B_{s, s-2}^{(1)}} \quad (17)$$

from Conditions 2 and 4.

Now, let us embed the ROCK1 or ROCK2 methods in (13). Then,  $A_{i_a i_b}^{(0)}$  and  $\alpha_{i_a}$  ( $1 \leq i_a \leq s$ ,  $1 \leq i_b < i_a$ ) are given by the Chebyshev formulation, which means

$$\mathbf{H}_i^{(0)} = K_{i-1} \quad (i = 1, 2, \dots, s), \quad \mathbf{y}_n + \sum_{i=1}^s \alpha_i h \mathbf{f}(\mathbf{H}_i^{(0)}) = K_s. \quad (18)$$

Because of the ROCK1 or ROCK2 methods, Condition 1 is automatically satisfied. All that remains is Condition 6. If (13) satisfies (18) with formulation (8), for a given  $s$  we call (13) an SROCKD1 method, whereas with formulation (9), we call it an SROCKD2 method.

#### 4. MS stability analysis

As with the deterministic case, the quality of a stochastic method can be partly characterized by its stability region, associated with the scalar linear test equation

$$dy(t) = \lambda y(t)dt + \sum_{j=1}^m \sigma_j y(t) dW_j(t), \quad t > 0, \quad y(0) = y_0, \quad (19)$$

where  $\lambda, \sigma_1, \dots, \sigma_m \in \mathbf{C}$  and where  $y_0 \neq 0$  with probability one (w. p. 1). The solution is MS stable ( $\lim_{t \rightarrow \infty} E[|y(t)|^2] = 0$ ) if

$$2\Re(\lambda) + \sum_{j=1}^m |\sigma_j|^2 < 0 \quad (20)$$

in the Itô case [17] or

$$\Re(\lambda) + \sum_{j=1}^m (\Re(\sigma_j))^2 < 0 \quad (21)$$

in the Stratonovich case [18].

Let us apply our SROCKD1 and SROCKD2 methods to (19). Due to (18) we can easily see that

$$H_i^{(0)} = P_{i-1}(h\lambda)y_n \quad (1 \leq i \leq s)$$

and

$$y_n + \sum_{i=1}^s \alpha_i h f(H_i^{(0)}) = P_s(h\lambda)y_n$$

for the SROCKD1 methods, whereas

$$H_i^{(0)} = Q_{i-1}(h\lambda)y_n \quad (1 \leq i \leq s-1), \quad H_s^{(0)} = (1 + h\lambda\theta_s)Q_{s-2}(h\lambda)y_n$$

and

$$y_n + \sum_{i=1}^s \alpha_i h f(H_i^{(0)}) = [1 + 2h\lambda\theta_s + (h\lambda)^2\tau_s] Q_{s-2}(h\lambda)y_n$$

for the SROCKD2 methods. Because of (15), we now successively compute  $H_i^{(j)}$  for  $i = s - 2, s - 1, s$  and  $y_{n+1}$ . Once we find the form

$$y_{n+1} = R_s \left( h, \lambda, \{\Delta W_j\}_{j=1}^m, \left\{ \tilde{\zeta}^{(l,j)} \right\}_{j,l=1}^m, \{\sigma_j\}_{j=1}^m \right) y_n,$$

the MS stability function will be given by

$$\hat{R}_s(p, q) = E \left[ \left| R_s \left( h, \lambda, \{\Delta W_j\}_{j=1}^m, \left\{ \tilde{\zeta}^{(l,j)} \right\}_{j,l=1}^m, \{\sigma_j\}_{j=1}^m \right) \right|^2 \right] \quad (22)$$

in the Itô case, and

$$\hat{R}_s(p, q, \tilde{q}) = E \left[ \left| R_s \left( h, \lambda, \{\Delta W_j\}_{j=1}^m, \left\{ \tilde{\zeta}^{(l,j)} \right\}_{j,l=1}^m, \{\sigma_j\}_{j=1}^m \right) \right|^2 \right] \quad (23)$$

in the Stratonovich case, where  $p \stackrel{\text{def}}{=} h\lambda$ ,  $q \stackrel{\text{def}}{=} \sum_{j=1}^m h|\sigma_j|^2$  and  $\tilde{q} \stackrel{\text{def}}{=} \sum_{j=1}^m h\sigma_j^2$ .

Thus, the MS stability domain of our methods are defined by  $\{(p, q) \mid \hat{R}_s(p, q) < 1\}$  in the Itô case or by  $\{(p, q, \tilde{q}) \mid \hat{R}_s(p, q, \tilde{q}) < 1\}$  in the Stratonovich case.

#### 4.1. MS stability function for SROCKD1 methods

Taking stability into account, let us assume

$$A_{s-2, i_b}^{(1)} = A_{s-1, i_b}^{(1)} = A_{s, i_b}^{(1)} = \alpha_{i_b} \quad (1 \leq i_b \leq s) \quad (24)$$

as this leads to

$$y_n + \sum_{i_b=1}^s A_{i_a i_b}^{(1)} h f \left( H_{i_b}^{(0)} \right) = P_s(h\lambda) y_n \quad (i_a = s - 2, s - 1, s)$$

when the SROCKD1 methods are applied to (19). Then, Condition 6 is automatically satisfied from Condition 3 and we have

$$\begin{aligned} & R_s \left( h, \lambda, \{\Delta W_j\}_{j=1}^m, \left\{ \tilde{\zeta}^{(l,j)} \right\}_{j,l=1}^m, \{\sigma_j\}_{j=1}^m \right) \\ &= \left( 1 + \sum_{j=1}^m \Delta W_j \sigma_j + \sum_{j,l=1}^m \sqrt{h} \sigma_j \tilde{\zeta}^{(l,j)} \sigma_l \right) P_s(h\lambda) \end{aligned}$$

Table 1: Optimal values of  $\eta_1$  for in the Itô (Stratonovich) case

$s$	$\eta_1$	$\tilde{l}_s^{(\eta_1)}$	$s$	$\eta_1$	$\tilde{l}_s^{(\eta_1)}$
3	4.3 (3.4)	6.7 (7.4)	6	8.1 (6.6)	18.9 (20.7)
9	10.9 (9.1)	35.9 (39.1)	15	15.1 (12.9)	83.3 (89.8)
26	20.1 (17.9)	212.3 (227.1)	53	29.2 (26.0)	736.5 (780.2)
74	34.0 (30.4)	1331.1 (1405.9)	104	39.1 (35.3)	2448.1 (2576.0)

by utilizing (16), (17) and (24).

Now, in order to seek the MS stability function, we calculate the expectation  $E|R_s|^2$  in the right-hand side of (22) or (23). Noting that

$$E[(\Delta W_j)^2] = h, \quad E\left[\left(\tilde{\zeta}^{(j,l)}\right)^2\right] = \frac{h}{2}$$

for  $j, l = 1, 2, \dots, m$  and the other expectations such as  $E\left[\Delta W_j \tilde{\zeta}^{(j,j)}\right]$  appearing in  $E|R_s|^2$  vanish for Itô SDEs, we obtain

$$\hat{R}_s(p, q) = \left(1 + q + \frac{1}{2}q^2\right) |P_s(p)|^2. \quad (25)$$

On the other hand, noting that

$$E\left[\tilde{\zeta}^{(j,j)}\right] = \frac{\sqrt{h}}{2}, \quad E[(\Delta W_j)^2] = h, \quad E\left[\left(\tilde{\zeta}^{(j,j)}\right)^2\right] = \frac{3h}{4}, \quad E\left[\left(\tilde{\zeta}^{(j,j)}\tilde{\zeta}^{(l,l)}\right)\right] = \frac{h}{4}$$

for  $j \neq l$  and the other expectations appearing in  $E|R_s|^2$  vanish for Stratonovich SDEs, we obtain

$$\hat{R}_s(p, q, \tilde{q}) = \left\{\left|1 + \frac{1}{2}\tilde{q}\right|^2 + q + \frac{1}{2}q^2\right\} |P_s(p)|^2. \quad (26)$$

As we have seen in (7),  $P_s(z)$  is given in explicit form. This fact makes it possible for us to arrange the value of  $\eta_1$ . Let us denote  $\Re(p)$  and  $\Im(p)$  by  $p_r$  and  $p_i$ , respectively. Similarly to [3], when  $p_i = 0$  we consider  $\tilde{l}_s^{(\eta_1)} > 0$  such that for all  $p_r \geq -\tilde{l}_s^{(\eta_1)}$ , the profile of the MS stability domain of the SROCKD1 methods includes the region where (20) or (21) is satisfied. In



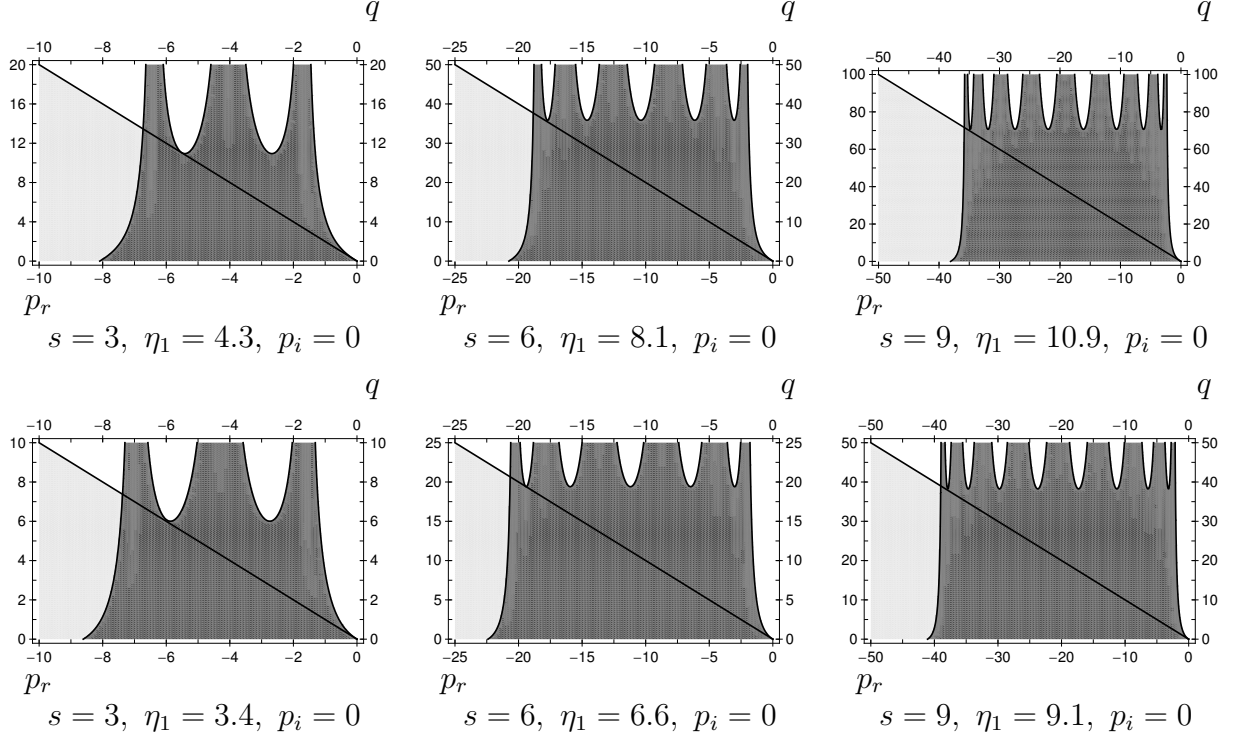


Figure 2: Profile of the MS stability domain of the SROCKD1 methods in the Itô case (top) and the Stratonovich case (bottom)

order to plot not only the profile but also the MS stability domain itself, we suppose

$$\Im(\sigma_j) = 0 \quad (j = 1, 2, \dots, m), \quad (27)$$

in the Stratonovich case because it leads to  $\tilde{q} = q$ . When we determine the values of  $\tilde{l}_s^{(\eta_1)}$  as large as possible, we obtain Table 1 by numerical calculations. Then, the profile of the MS stability domain of the SROCKD1 methods is given in Figure 2. In the figure the dark-colored area indicates the profile of the MS stability domain when  $p_i = 0$ , whereas the area enclosed by the two straight lines  $q = 0$  and  $q = -2p_r$  or  $q = -p_r$  indicates the region in which the solution of the test SDE is MS stable. Thus, the light-colored area indicates the region in which the solution of the test SDE is MS stable, but which is not included in the MS stability domain.

Table 2: Value of $\frac{T_s''(1)T_s(1)}{(T_s'(1))^2}$							
$s$	3	6	9	20	50	100	200
$\frac{T_s''(1)T_s(1)}{(T_s'(1))^2}$	$\frac{8}{27}$	$\frac{35}{108}$	$\frac{80}{243}$	$\frac{133}{400}$	$\frac{833}{2500}$	$\frac{3333}{10000}$	$\frac{13333}{40000}$

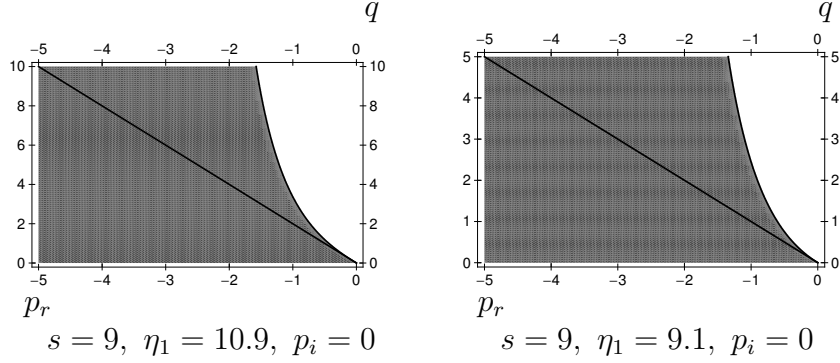


Figure 3: Magnified profile of the MS stability domain of the SROCKD1 methods in the Itô case (left) and the Stratonovich case (right)

Incidentally, the curve satisfying  $\hat{R}_s(p, q) = 1$  gives the boundary of the MS stability domain in the Itô case. Thus from (25)

$$\left(1 + q + \frac{1}{2}q^2\right) (P_s(p_r))^2 = 1 \quad (28)$$

represents the boundary of the profile for the SROCKD1 methods when  $p_i = 0$ . By differentiating both sides of (28) with respect to  $p_r$  and substituting  $p_r = q = 0$ , we obtain

$$\frac{dq}{dp_r}(0) = -2.$$

Hence, the slope of the boundary curve at the origin  $(p_r, q) = (0, 0)$  is equal to that of the straight line  $q = -2p_r$ . Further, similarly, we have

$$\frac{d^2q}{dp_r^2}(0) = 2 - 2\frac{d^2P_s}{dp_r^2}(0).$$

Here,

$$\frac{d^2P_s}{dp_r^2}(0) = \frac{T_s''(\omega_0)T_s(\omega_0)}{(T_s'(\omega_0))^2}$$

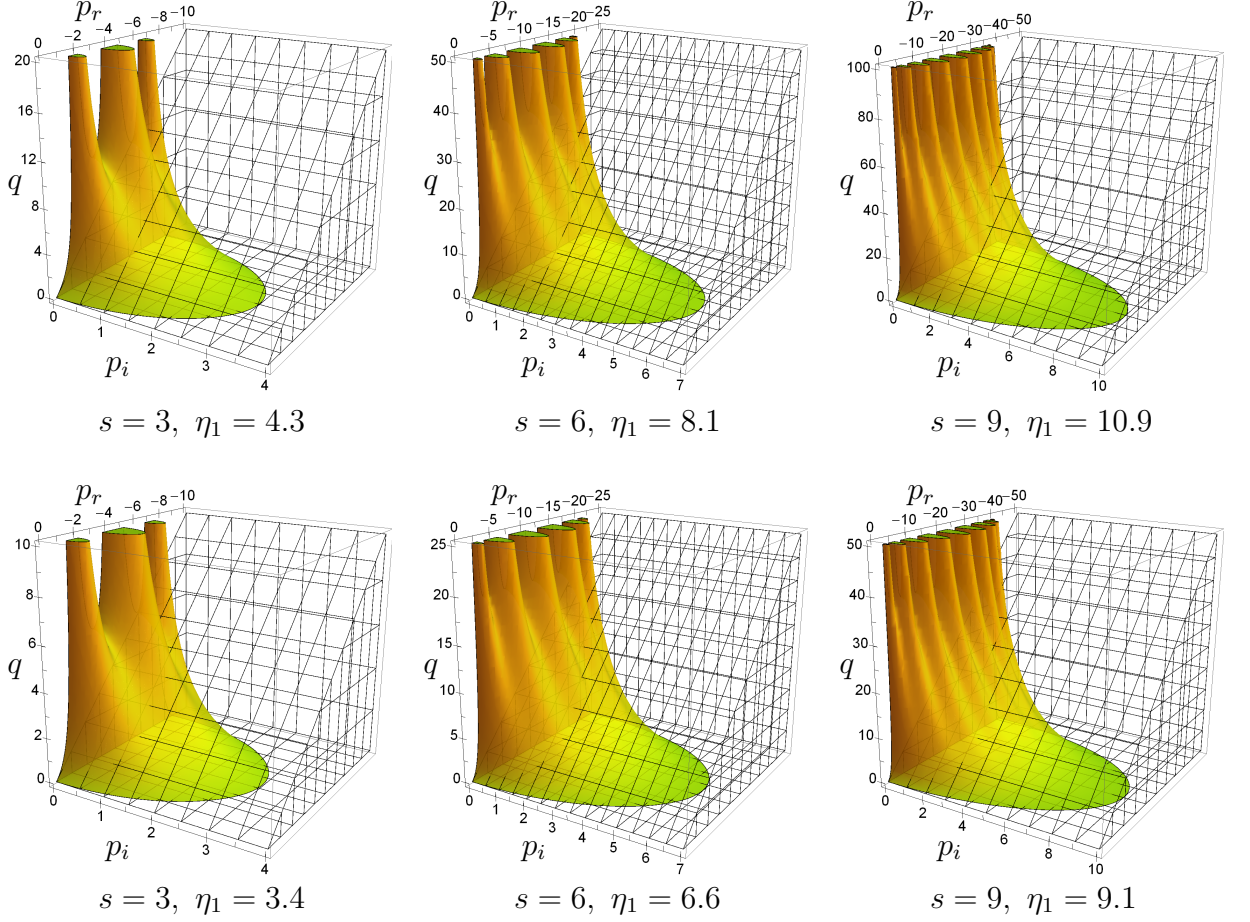


Figure 4: MS stability domain of the SROCKD1 methods in the Itô case (top) and the Stratonovich case (bottom)

from (7). If we calculate the expression in the right-hand side for  $\omega_0 = 1$ , we have

$$0 < \frac{T_s''(1)T_s(1)}{(T_s'(1))^2} < \frac{1}{3} \quad (3 \leq s \leq 200).$$

Some of these values are given in Table 2. Thus, we can see that  $\frac{d^2q}{dp_r^2}(p_r) > 0$  for  $p_r \in [-\varepsilon_1, 0]$  if  $0 < \eta_1/s^2 < \varepsilon_2$  ( $\varepsilon_1, \varepsilon_2$ : small positive values), which means  $1 < \omega_0 < 1 + \varepsilon_2$ . Consequently, the boundary curve does not cross the line  $q = -2p_r$  and its slope is smaller than  $-2$  near the origin  $(p_r, q) = (0, 0)$  when  $p_r$  is negative and  $\eta_1/s^2$  is small. A similar result is obtained for (26)

- see Figure 3.

Finally, we show the MS stability domain of the SROCKD1 methods in Figure 4. Because the domain is symmetrical with respect to the plane  $p_i = 0$ , we plot it only for  $p_i \geq 0$ . It is indicated with the colored part in the figure. The other part enclosed by mesh indicates the domain in which the solution of the test SDE is MS stable.

#### 4.2. MS stability function for SROCKD2 methods

Taking stability into account, we assume

$$\begin{aligned} A_{s-2,i_b}^{(1)} &= A_{s-1,i_b}^{(1)} = A_{s,i_b}^{(1)} = A_{s-1,i_b}^{(0)} \quad (1 \leq i_b \leq s-2), \\ A_{s-2,i_b}^{(1)} &= A_{s-1,i_b}^{(1)} = A_{s,i_b}^{(1)} = 0 \quad (i_b = s-1, s) \end{aligned} \quad (29)$$

and this leads to

$$y_n + \sum_{i_b=1}^s A_{i_a i_b}^{(1)} h f \left( H_{i_b}^{(0)} \right) = Q_{s-2}(h\lambda) y_n \quad (i_a = s-2, s-1, s)$$

when the SROCKD2 methods are applied to (19). Then, Condition 6 is automatically satisfied from Condition 3 and we have

$$\begin{aligned} R_s \left( h, \lambda, \{\Delta W_j\}_{j=1}^m, \left\{ \tilde{\zeta}^{(l,j)} \right\}_{j,l=1}^m, \{\sigma_j\}_{j=1}^m \right) \\ = \left\{ 1 + 2\theta_s h\lambda + \tau_s (h\lambda)^2 + \sum_{j=1}^m \Delta W_j \sigma_j + \sum_{j,l=1}^m \sqrt{h} \sigma_j \tilde{\zeta}^{(l,j)} \sigma_l \right\} Q_{s-2}(h\lambda) \end{aligned}$$

by utilizing (16), (17) and (29). Similarly to the previous subsection, thus, we obtain

$$\hat{R}_s(p, q) = \left\{ |1 + 2\theta_s p + \tau_s p^2|^2 + q + \frac{1}{2} q^2 \right\} |Q_{s-2}(p)|^2$$

in the Itô case and

$$\hat{R}_s(p, q, \tilde{q}) = \left\{ \left| 1 + 2\theta_s p + \tau_s p^2 + \frac{1}{2} \tilde{q} \right|^2 + q + \frac{1}{2} q^2 \right\} |Q_{s-2}(p)|^2$$

in the Stratonovich case.

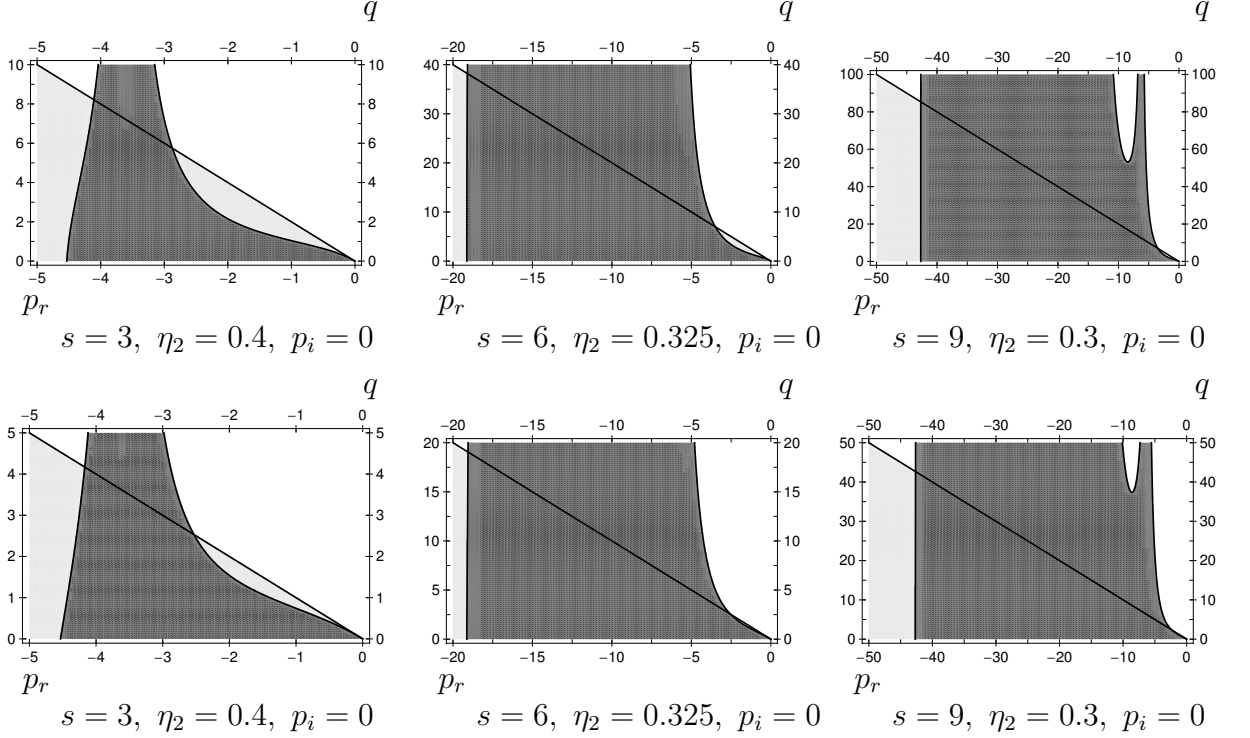


Figure 5: Profile of the MS stability domain of the SROCKD2 methods in the Itô case (top) and the Stratonovich case (bottom)

As we have seen in Subsection 2.2, in order to obtain the values of  $\theta_s$  and  $\tau_s$ , we have to decide the values of  $\alpha_s$ ,  $\beta_s$ ,  $a_s$  and  $l_s$  for a given  $\eta_2$  and  $s$ . The numerical algorithm [2] to do it is very time consuming if  $\eta_2$  is small. Thus, we set a moderately small value at  $\eta_2$  for each  $s$  and we decide the parameter values of  $\alpha_s$ ,  $\beta_s$ ,  $a_s$  and  $l_s$ . Now, in order to plot not only the profile but also the MS stability domain, let us suppose (27) holds in the Stratonovich case as it leads to  $\tilde{q} = q$ . Then, the profile of the MS stability domain of the SROCKD2 methods is given in Figure 5.

In Figure 6, the magnified profile of the MS stability domain is indicated for the SROCKD2 methods with  $s = 9$ . Here, again the light-colored area indicates the region in which the solution of the test SDE is MS stable, but which is not included in the MS stability domain. It should be noted that such a region appears along the line  $q = -2p_r$  or  $q = -p_r$  for large  $p_r < 0$ .

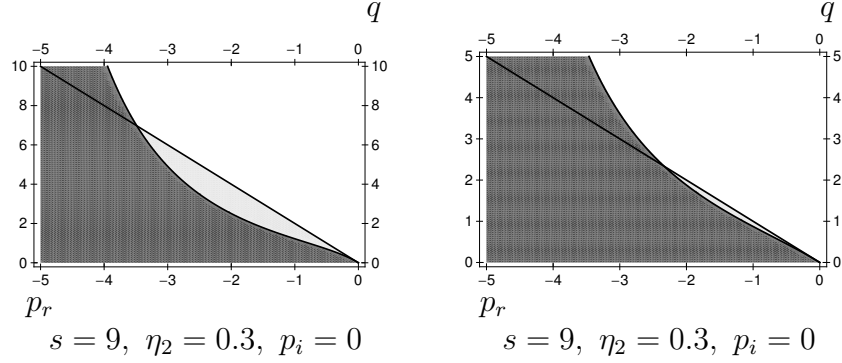


Figure 6: Magnified profile of the MS stability domain of the SROCKD2 methods in the Itô case (left) and the Stratonovich case (right)

This is one of the critical differences between SROCKD1 and SROCKD2 methods. Finally, we show the MS stability domain of SROCKD2 methods in Figure 7.

#### 4.3. MS stability analysis for other schemes

In this subsection, we briefly investigate MS stability properties for two types of schemes. One is the family of SROCK schemes proposed by Abdulle and Li [4], which is of strong order a half for non-commutative Itô SDEs. The other is the SRI1 scheme proposed by Rößler [12], which is of strong order one for non-commutative Itô SDEs. By numerical experiments in the next section, we will compare our numerical schemes with these schemes.

When the SROCK schemes are applied to (19), similarly to [4] we obtain

$$\hat{R}_s(p, q) = |P_s(p)|^2 + q |P_{s-1}(p)|^2$$

because

$$R_s \left( h, \lambda, \{\Delta W_j\}_{j=1}^m, \{\sigma_j\}_{j=1}^m \right) = P_s(h\lambda) + \sum_{j=1}^m \Delta W_j \sigma_j P_{s-1}(h\lambda).$$

Here, note that the common  $\omega_0$  and  $\omega_1$  have to be used in calculations of  $P_s(p)$  and  $P_{s-1}(p)$ :  $\omega_0 = 1 + \frac{\eta_1}{s^2}$  and  $\omega_1 = \frac{T_s(\omega_0)}{T'_s(\omega_0)}$ . On the other hand, when the SRI1 scheme is applied to (19), we obtain

$$\hat{R}_s(p, q) = |1 + p|^2 + q + \frac{1}{2}q^2$$

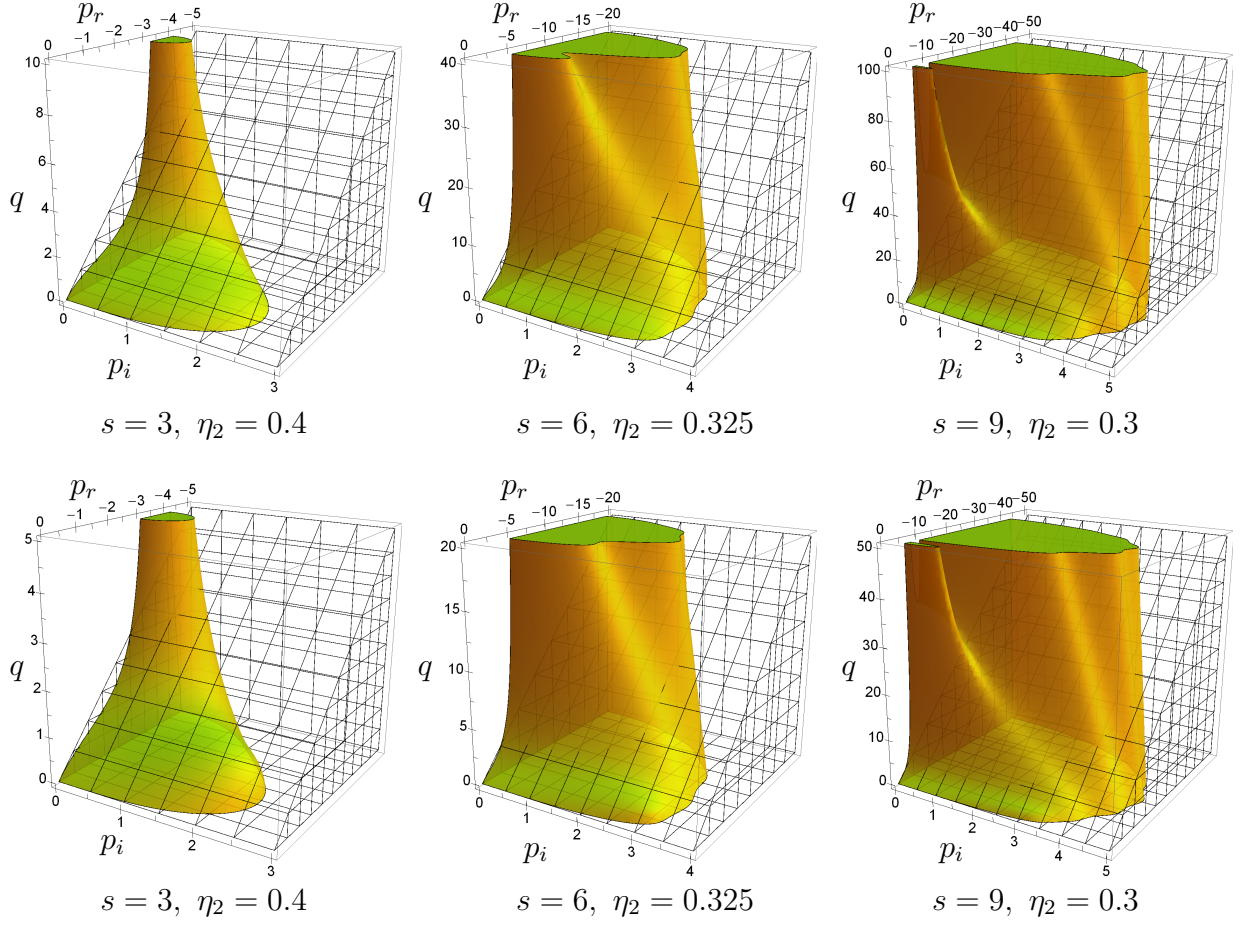


Figure 7: MS stability domain of the SROCKD2 methods in the Itô case (top) and the Stratonovich case (bottom)

because

$$\begin{aligned}
R_s & \left( h, \lambda, \{\Delta W_j\}_{j=1}^m, \left\{ \tilde{\zeta}^{(l,j)} \right\}_{j,l=1}^m, \{\sigma_j\}_{j=1}^m \right) \\
& = 1 + h\lambda + \sum_{j=1}^m \Delta W_j \sigma_j + \sum_{j,l=1}^m \sqrt{h} \sigma_j \tilde{\zeta}^{(l,j)} \sigma_l.
\end{aligned}$$

The MS stability domain and its profile are indicated in Figures 8 and 9 for the SROCK schemes and the SRI1 scheme, respectively.

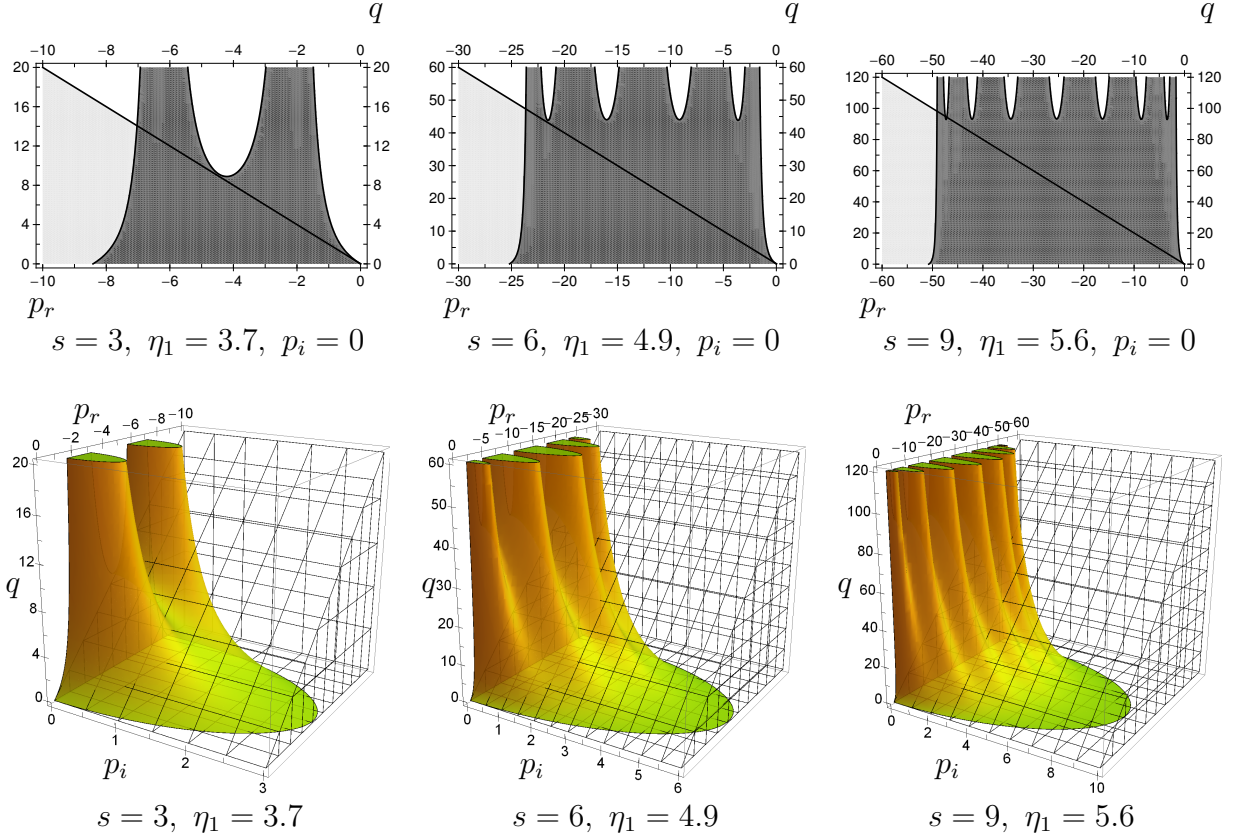


Figure 8: MS stability domain (bottom) and its profile (top) of the SROCK schemes

## 5. Numerical experiments

In Section 3 we have derived SROCKD1 and SROCKD2 methods, which have the free parameters  $B_{s-1,s-2}^{(1)}$ ,  $B_{s,s-2}^{(1)}$  and  $\beta_{s-2}^{(1)}$ . Now, for simple parameter values in (16) and (17), let us set them as follows:

$$B_{s-1,s-2}^{(1)} = -B_{s,s-2}^{(1)} = \beta_{s-2}^{(1)} = 1$$

and confirm the performance of the schemes in numerical experiments. In the sequel, we investigate the root mean square error (RMSE) by simulating 2000 independent trajectories for a given  $h$ . We also investigate computational costs. In simulation results, we will indicate  $S_a \stackrel{\text{def}}{=} n_e d + n_r$ , where  $n_e$  and  $n_r$



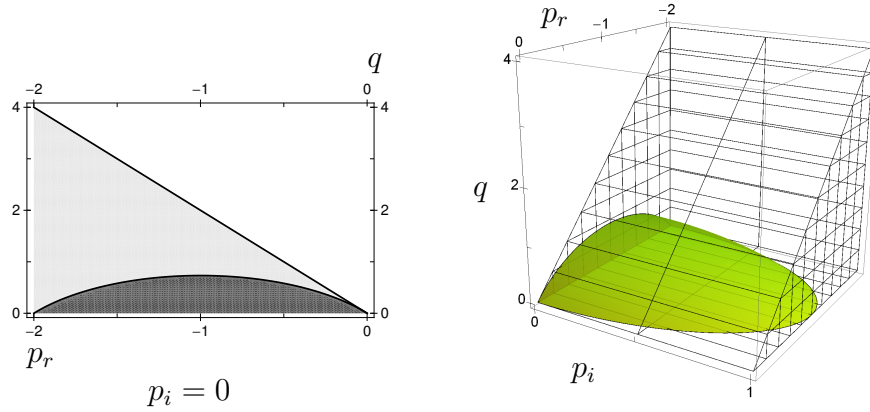


Figure 9: MS stability domain (right) and its profile (left) of the SRI1 scheme

stand for the number of evaluations on the drift or diffusion coefficients and the number of generated pseudo random numbers, respectively.

The first example is a nonlinear two-dimensional Itô SDE with a four-dimensional Wiener process [12]:

$$\begin{aligned}
 d\mathbf{y}(t) = & \mathbf{y}(t)dt + \begin{bmatrix} \cos(\frac{1}{2}) \\ \sin(\frac{1}{2}) \end{bmatrix} \sin(y_1(t))dW_1(t) + \begin{bmatrix} \cos(\frac{1}{2}) \\ \sin(\frac{1}{2}) \end{bmatrix} \cos(y_1(t))dW_2(t) \\
 & + \begin{bmatrix} -\sin(\frac{1}{2}) \\ \cos(\frac{1}{2}) \end{bmatrix} \sin(y_2(t))dW_3(t) + \begin{bmatrix} -\sin(\frac{1}{2}) \\ \cos(\frac{1}{2}) \end{bmatrix} \cos(y_2(t))dW_4(t), \\
 t > 0, \quad & \mathbf{y}(0) = [2 \ 2]^\top \quad (\text{w. p. } 1).
 \end{aligned} \tag{30}$$

As the SROCKD1 and SROCKD2 schemes, as well as the SRI1 scheme, need approximations to stochastic double integrals, we use the algorithm proposed by Wiktorsson [13]. In addition, because we do not know the exact solution of (30), we seek a numerical solution with  $h = 2^{-12}$  by the SRI1 scheme and use it instead of the exact solution.

The results are indicated in Figure 10. In the sequel, if a solution is a vector, the Euclidean norm is used. The solid, dash, dotted or dash-dotted lines denote the SROCKD2 scheme with three stages ( $\eta_2 = 0.375$ ), the SROCKD1 scheme with three stages ( $\eta_1 = 4.3$ ), the SRI1 scheme or the SROCK scheme with three stages ( $\eta_1 = 3.7$ ), respectively. We can see that the SROCKD2 scheme is the best not only in the root mean square errors

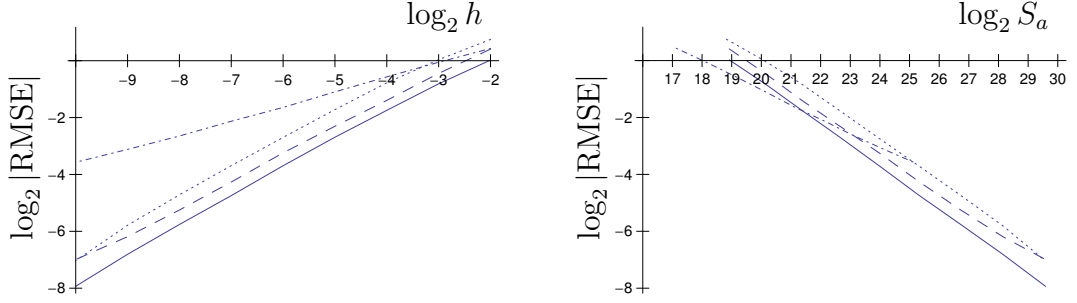


Figure 10: RMSEs of  $\mathbf{y}(1)$ . (Solid: SROCKD2, dash: SROCKD1, dotted: SRI1, dash-dotted: SROCK.)

(RMSEs), but also in the computational costs. Here, remember that the SROCK scheme is of strong order a half, whereas the other three schemes are of strong order one.

The second example comes from the heat equation with noise [3]:

$$\begin{aligned} du(t, x) &= \Delta u(t, x)dt + \sigma_1 \sin(u(t, x))dW_1(t) + \sigma_2 u(t, x) \cos(u(t, x))dW_2(t), \\ (t, x) &\in [0, T] \times [0, 1]. \end{aligned} \tag{31}$$

Here,  $\Delta$  is the Laplacian operator, and  $\sigma_1$  and  $\sigma_2$  are noise parameters. As usual,  $W_1(t)$  and  $W_2(t)$  stand for independent Wiener processes.

Take  $u(0, x) = 0.1$  as an initial condition and  $u(t, 0) = \frac{\partial u(t, x)}{\partial x}|_{x=1} = 0$  as mixed boundary conditions. If we discretize the space interval by  $N + 1$  equidistant points  $x_i$  ( $0 \leq i \leq N$ ) and define a vector-valued function by  $\mathbf{y}(t) \stackrel{\text{def}}{=} [u(t, x_1) \ u(t, x_2) \ \cdots \ u(t, x_N)]^\top$ , then we obtain

$$\begin{aligned} d\mathbf{y}(t) &= A\mathbf{y}(t)dt + \sigma_1 \mathbf{b}_1(\mathbf{y}(t))dW_1(t) + \sigma_2 \mathbf{b}_2(\mathbf{y}(t))dW_2(t), \quad t > 0, \\ \mathbf{y}(0) &= [0.1 \ 0.1 \ \cdots \ 0.1]^\top \quad (\text{w. p. } 1) \end{aligned} \tag{32}$$

by applying the central difference scheme to (31) and by using the relationship

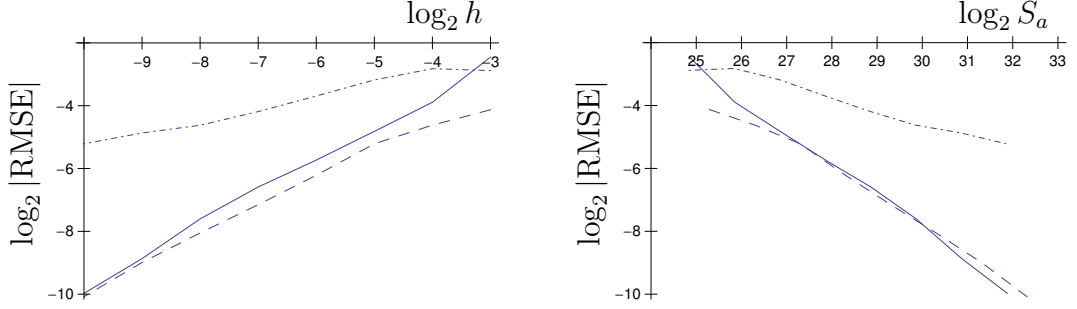


Figure 11: RMSEs of  $\mathbf{y}(1)$ . (Solid: SROCKD2, dash: SROCKD1, dash-dotted: SROCK.)

$u(t, x_{N-1}) = u(t, x_{N+1})$  from the boundary conditions, where

$$A \stackrel{\text{def}}{=} N^2 \begin{bmatrix} -2 & 1 & & & 0 \\ 1 & -2 & 1 & & \\ & \ddots & \ddots & \ddots & \\ 0 & & 1 & -2 & 1 \\ & & & 2 & -2 \end{bmatrix}, \quad \mathbf{b}_1(\mathbf{y}) \stackrel{\text{def}}{=} \begin{bmatrix} \sin(y_1) \\ \sin(y_2) \\ \vdots \\ \sin(y_N) \end{bmatrix},$$

$$\mathbf{b}_2(\mathbf{y}) \stackrel{\text{def}}{=} \begin{bmatrix} y_1 \cos(y_1) \\ y_2 \cos(y_2) \\ \vdots \\ y_N \cos(y_N) \end{bmatrix}.$$

The linearized SDE centered at  $\mathbf{y} = \mathbf{0}$  for (32) is

$$\begin{aligned} d\mathbf{y}(t) &= A\mathbf{y}(t)dt + \sigma_1\mathbf{y}(t)dW_1(t) + \sigma_2\mathbf{y}(t)dW_2(t), \quad t > 0, \\ \mathbf{y}(0) &= [0.1 \ 0.1 \ \cdots 0.1]^\top \quad (\text{w. p. } 1). \end{aligned} \tag{33}$$

If we calculate the eigenvalues of  $A$ , we can see that they are distributed in the interval  $(-4N^2, -2.3)$  for  $N \geq 2$  [3]. Thus, let us assume  $\sigma_1 = \sigma_2 = \sqrt{2}$  because then the solution of (33) is MS stable. On the other hand, note that standard explicit SRK schemes need a very small step size for stability when  $N$  is large.

Let us assume  $N = 40$ . Because we do not know the exact solution of (32), we seek a numerical solution by the SRI1 scheme with  $h = 2^{-14}$  and use it instead of the exact solution.

Some results are given in Figure 11. The solid, dash or dash-dotted lines denote the SROCKD2 scheme with 41 stages ( $\eta_2 = 0.285$ ), the SROCKD1 scheme with 58 stages ( $\eta_1 = 32.7$ ), or the SROCK scheme with 45 stages ( $\eta_1 = 10.3$ ), respectively. These stage numbers have been used such that each scheme can solve (32) numerically stably with  $h = 2^{-3}$ . Note that the SROCKD1 scheme with 41, 45 or 53 stages and the SROCK scheme with 41 stages cannot solve it for  $h = 2^{-3}$  even if  $\sigma_1 = \sigma_2 = 0$ , because the MS stability domain of the SROCK or SROCKD1 methods is shorter along the negative axis of  $p_r$  than that of the SROCKD2 methods when they have the same stage number and it is large. From Figure 11, we can see that the SROCKD1 and SROCKD2 schemes are superior to the SROCK schemes due to the latter's low convergence order. Incidentally, the SRI1 scheme cannot solve (32) numerically stably with  $h = 2^{-i}$  ( $1 \leq i \leq 11$ ). When  $h = 2^{-12}$ , it gives  $\log_2 |\text{RMSE}| = -12.0$  and  $\log_2 S_a = 31.5$  and is computationally efficient for this step size. Thus, we can see that the SROCKD1 and SROCKD2 schemes have good performance not only with respect to stability, but also in terms of computational costs.

## 6. Concluding remarks

For non-commutative Itô and Stratonovich SDEs, we have derived explicit  $s$ -stage strong first order SROCKD1 and SROCKD2 schemes, which are of order one and two for ODEs, respectively. As the ROCK1 or ROCK2 methods with a damping factor are embedded in these methods, they have a large MS stability domain along the negative axis of  $p_r$  when  $p_i = 0$ . In the case of the SROCKD1 schemes, optimal damping values have been chosen. In addition, because the schemes are based on efficient SRK methods in [12], we can expect they are efficient in terms of not only the number of generated pseudo random numbers but also in the number of evaluations on the diffusion coefficients. The MS stability domain of these methods have also been studied in both the Itô and Stratonovich cases.

In the numerical experiments we have confirmed the advantages of these methods. In the first numerical example, we have investigated four schemes with three stages and have seen an advantage of our schemes in terms of computational costs. The second example has highlighted the advantages of our schemes in terms of accuracy and stability. In other words, whereas the SRI1 scheme or the SROCK scheme have suffered from poor stability

properties or low convergence order, respectively, our schemes have shown high performance in accuracy, computational costs and stability.

Finally, we should make the following remarks. Recently, Buckwar and Kelly [19] and Buckwar and Sickenberger [20] have proposed MS stability analyses for systems of Itô SDEs. However, some of their analyses require extensive algebraic and possibly symbolic calculations. Most of the construction of our methods has required intensive numerical searching and to follow this new approach would require an additional complexity that would substantially increase the length of the paper and be beyond the scope of the paper's original intention. However, we will consider these issues in future work.

## Acknowledgments

The authors would like to thank the referees for their valuable comments which helped to improve the earlier versions of this paper. This work was partially supported by JSPS Grant-in-Aid for Scientific Research No. 23540143.

## References

- [1] P. van der Houwen, B. Sommeijer, On the internal stability of explicit  $m$ -stage Runge-Kutta methods for large  $m$ -values, *Z. Angew. Math. Mech.* **60** (1980) 479–485.
- [2] A. Abdulle, A. Medovikov, Second order Chebyshev methods based on orthogonal polynomials, *Numer. Math.* **90** (2001) 1–18.
- [3] A. Abdulle, S. Cirilli, S-ROCK: Chebyshev methods for stiff stochastic differential equations, *SIAM J. Sci. Comput.* **30** (2008) 997–1014.
- [4] A. Abdulle, T. Li, S-ROCK methods for stiff Itô SDEs, *Commun. Math. Sci.* **6** (2008) 845–868.
- [5] J. Alcock, K. Burrage, A note on the Balanced method, *BIT* **46** (2006) 689–710.
- [6] K. Burrage, L. Lenane, G. Lythe, Numerical methods for second-order stochastic differential equations, *SIAM J. Sci. Comput.* **29** (2007) 245–264.

- [7] P. Kloeden, E. Platen, Numerical Solution of Stochastic Differential Equations, Springer-Verlag, New York, 1999. Corrected Third Printing.
- [8] G. Milstein, E. Platen, H. Schurz, Balanced implicit methods for stiff stochastic systems, SIAM J. Appl. Math. **35** (1998) 1010–1019.
- [9] H. Schurz, The invariance of asymptotic laws of linear stochastic systems under discretization, Z. Angew. Math. Mech. **79** (1999) 375–382.
- [10] K. Burrage, P. Burrage, Order conditions of stochastic Runge-Kutta methods by B-series, SIAM J. Numer. Anal. **38** (2000) 1626–1646.
- [11] J. Butcher, Numerical Methods for Ordinary Differential Equations, John Wiley & Sons, Chichester, second edition, 2008.
- [12] A. Rößler, Runge-Kutta methods for the strong approximation of solutions of stochastic differential equations, SIAM J. Numer. Anal. **48** (2010) 922–952.
- [13] M. Wiktorsson, Joint characteristic function and simultaneous simulation of iterated Itô integrals for multiple independent Brownian motions, The Annals of Prob. **11** (2001) 470–487.
- [14] Y. Komori, K. Burrage, Weak second order S-ROCK methods for Stratonovich stochastic differential equations, J. Comput. Appl. Math. **236** (2012) 2895–2908.
- [15] W. Riha, Optimal stability polynomials, Computing **9** (1972) 37–43.
- [16] L. Arnold, Stochastic Differential Equations: Theory and Applications, John Wiley & Sons, New York, 1974.
- [17] D. Higham, A-stability and stochastic mean-square stability, BIT **40** (2000) 404–409.
- [18] Y. Komori, T. Mitsui, Stable ROW-type weak scheme for stochastic differential equations, Monte Carlo Methods and Appl. **1** (1995) 279–300.
- [19] E. Buckwar, C. Kelly, Towards a systematic linear stability analysis of numerical methods for systems of stochastic differential equations, SIAM J. Numer. Anal. **48** (2010) 298–321.

- [20] E. Buckwar, T. Sickenberger, A structural analysis of mean-square stability for multi-dimensional linear stochastic differential systems, Appl. Numer. Math. **62** (2012) 842–859.